Received Date : 19-Sep-2016
Revised Date : 03-Dec-2016
Accepted Date : 05-Dec-2016
Article type : Article
Co-ordinating Editor : Bernard Raveau

Ferroic ordering and charge-spin-lattice order coupling in Gd-doped Fe_3O_4 nanoparticles relaxor multiferroic system

Suvra S. Laha[1,#],Ehab Abdelhamid[1,$], Maheshika P. Arachchige[1], Ajay Kumar[1] and Ambesh Dixit[2,*]

[1]Department of Physics and Astronomy, Wayne State University, Detroit, MI, USA
[2]Department of Physics & Center for Solar Energy, Indian Institute of Technology Jodhpur,INDIA

ABSTRACT

We investigated the effect of gadolinium doping (1-5 *at.%*) on the magnetic and dielectric properties of Fe_3O_4 nanoparticles, synthesized by the chemical co-precipitation technique, primarily to understand the onset of multifunctional properties such as ferroelectricity and magnetodielectric coupling. The substitution of larger Gd^{3+} ions at smaller Fe^{3+} octahedral sites in inverse spinel Fe_3O_4 has significantly influenced the morphology, average crystallite size and more importantly, the magneto-crystalline anisotropy and saturation magnetization. The magneto-crystalline anisotropy and the saturation magnetization decreases substantially,

however, significant increase in the average crystallite size is observed upon Gd doping. Furthermore, temperature dependent dielectric studies suggest that these nanoparticle systems exhibit relaxor ferroelectric behavior, with much pronounced ferroelectric polarization moment recorded for 5 *at.%* Gd doped Fe_3O_4 as compared to its undoped counterpart.

Corresponding author E-mail: *ambesh@iitj.ac.in, #laha@wayne.edu, $du9779@wayne.edu

Authors Suvra S Laha and Ehab Abdelhamid contributed equally for this work

I. INTRODUCTION

Iron oxide and its derivative nanoparticle systems have attracted considerable attention because of their potential applications ranging from magnetic recording to cancer research[1, 2]. There are numerous studies performed on undoped and doped Fe_3O_4 nanoparticle systems[3-8], and also on magnetite-based nanocomposites [9-11] in an attempt to tune their magnetic and dielectric properties for effective technological and biomedical applications. In conjunction with such technological potentials, there are several unanswered questions regarding their physical properties such as Verwey transition (a transition between conducting and insulation state at Verwey transition temperature T_V (~122K) where Fe_3O_4 exhibits conducting state above T_V and insulating state below T_V), the onset of ferroelectricity, and magnetodielectric coupling as a function of crystallite geometries and doping in Fe_3O_4 matrix. Among these, Verwey transition is very sensitive to the stoichiometry of Fe_3O_4 system and is usually not observed in defective or non-stoichiometric samples. The relatively larger rare-earth ions have been used for doping in inverse spinel systems to induce strain modulated physical properties useful for magneto-optical recording [12], MRI contrast agents [13] etc. For example, the doping of Gd^{3+} into the inverse spinel cobalt ferrite prepared through different synthetic routes has altered the average crystallite size, lattice constants and more importantly the magnetic properties[14, 15]. Till date, prominent studies conducted on gadolinium–doped magnetite nanoparticles (GdFO) are focused on the lattice site modification using Gd^{3+} dopant in the spinel structure[16], their respective low-temperature magnetic properties[17] and related biomedical applications [8, 13]. Furthermore, the presence of heavy metal Gd ion with a highly magnetic Fe ion could possibly make GdFO a better candidate

for multimodal imaging purposes[18, 19]. The simultaneous presence of more than one functional property in GdFO nanomaterials may provide the additional degree of freedom, which can be used as an external controlling stimulus for the desired applications. In the present study, we aimed for investigating the effect of gadolinium doping on the magnetic, dielectric, ferroelectric and magnetodielectric properties of Fe_3O_4 nanoparticles. We observed that the substitution of Gd^{3+} ions at Fe^{3+} sites in Fe_3O_4 matrix has significantly influenced the average crystallite size, the saturation magnetization, dielectric and ferroelectric properties. The average crystallite size, estimated from x-ray diffraction (XRD) using Scherrer equation, increases with increasing Gd doping fraction and the saturation magnetization drops monotonically in the presence of excess Gd^{3+} ions. Interestingly, GdFO develops enhanced ferroelectric ordering at low temperatures. The details of the temperature dependent dielectric, ferroelectric and magnetodielectric measurements are discussed to understand the onset of charge-spin-lattice coupling in Gd-doped Fe_3O_4 system.

II. EXPERIMENTAL DETAILS

The undoped (denoted by FO) and GdFO nanoparticles were synthesized using the chemical co-precipitation technique[17], with $GdCl_3.6H_2O$ serving as the dopant material. Aqueous solutions of $FeCl_3 \cdot 6H_2O$, $FeCl_2 \cdot 4H_2O$, and $GdCl_3 \cdot 6H_2O$ were mixed in a beaker in a molar ratio of 1.85:1.00:0.15 to synthesize 5 *at.%* GdFO nanoparticles. Initially, $GdCl_3 \cdot 6H_2O$ was added to the $FeCl_3 \cdot 6H_2O$ solution, dissolved in deionized water and then after few minutes of stirring, an aqueous solution containing $FeCl_2 \cdot 4H_2O$ was poured into it. If the sequence, in which these salts are added, is altered, the saturation magnetization of these nanoparticles may get affected [17]. The entire reaction was carried out in N_2 atmosphere in order to avoid the partial oxidation of Fe^{2+} to α-FeOOH as found in a previous study [17]. For the preparation of 1 *at.%* and 2.5 *at.%* GdFO nanoparticles, $FeCl_3 \cdot 6H_2O$, $FeCl_2 \cdot 4H_2O$ and $GdCl_3 \cdot 6H_2O$ were mixed in molar ratios of 1.97:1.00:0.03 and 1.925:1.00:0.075 respectively and the same procedure[17] was adopted for sequential mixing. For simplicity, the 1, 2.5 and 5 *at.%* GdFO nanoparticles are marked as 1GdFO, 2.5GdFO, and 5GdFO respectively for later discussions.

III. RESULTS AND DISCUSSION

The XRD spectra (Figure 1(a)) on undoped and GdFO powder samples were performed using a Rigaku MiniFlex 600 x-ray diffractometer ($CuK\alpha_1$ radiation). All the observed diffraction peaks are indexed (JCPDS card number: 85-1436), suggesting the formation of phase-pure inverse spinel crystal structure of Fe_3O_4. Most likely, Gd^{3+} ions (ionic radii ~ 0.093 nm) are replacing the Fe^{3+} ions (ionic radii ~ 0.064 nm) of the octahedral sites in inverse spinel Fe_3O_4 [16]. Additionally, the XRD spectra suggest that doping of gadolinium does not have any significant impact on the crystal structure of Fe_3O_4. The refinement of XRD diffraction data does not reflect the presence of other crystallographic phase and only the observed inverse spinel phase explains the substitution of Gd into Fe sites. The average crystallite sizes estimated using Scherrer equation [17] are approximately 12 nm, 11.5 nm, 13.5 nm and 18 nm for FO, 1GdFO, 2.5GdFO and 5GdFO samples respectively. This increase in crystallite size suggests that crystals grow larger following an increase in the Gd doping percentage, an observation which has been also reported by Peng *et al.* on Gd-doped $CoFe_2O_4$ spinel nanoparticles [12]. The increased particle size is essentially a consequence of stress-induced effect primarily caused by the doping of a higher concentration of large Gd^{3+} ions at the smaller Fe^{3+} ion sites[12]. The Rietveld refined lattice parameters (*a*) are evaluated to be 8.381Å, 8.396 Å, 8.375 Å and 8.365 Å for FO, 1GdFO, 2.5GdFO and 5GdFO samples respectively[17]. The reduction in lattice parameter has been attributed to the Gd mediated strain in GdFeO samples.

For careful probing of nanostructures' morphology, transmission electron microscopy (JEOL-2010 FasTEM, 200kV) measurements were conducted on FO and 5GdFO samples (Figure 1(b)). It is observed that the particle morphology is susceptible to Gd doping, with nearly spherical structures representing undoped nanoparticles has assumed cubical or rhombohedral geometries in the case of Gd-doped sample (5GdFO). This variation in particle morphology is consistent with previous studies[8, 17], where such changes have been realized for even less than 1 *at.%* GdFO nanoparticles[8].The average size of FO particles obtained from TEM analysis is reported to be 13.2 nm with a standard deviation,σ=2.3 nm. The slight increase in the size of the particles observed in TEM as compared to XRD confirms the formation of a thin amorphous layer (~1 nm) on the surface of these nanoparticles[17]. Such determination of average particle size from the TEM images could not be achieved due to substantial clustering or agglomeration for the case of 5GdFO nanoparticles. The energy dispersive spectroscopy (EDS) measurements (not

shown) confirmed the excess gadolinium atomic fraction in 1GdFO, 2.5GdFO, and 5GdFO samples to be approximately 1.3, 3.0 and 5.5 *at.%* respectively. The microscopic measurements substantiate the observation for non-spherical particle morphology for 1GdFO, 2.5GdFO and 5GdFO samples.

The *dc* and *ac* characterizations of these nanoparticles were performed using a Quantum Design physical property measurement system (PPMS) for understanding the magnetic relaxation dynamics of these systems.The room temperature magnetization (M) *vs* magnetic field (H) data for all the samples are shown in Figure 2(a).The observed sigmoidal shape of these curves with nearly zero hysteresis confirms the superparamagnetic nature of these nanoparticles. The measured saturation magnetization (M_S) values are 65 emu/g, 51 emu/g and 45.5 emu/g for 1GdFO, 2.5GdFO and 5GdFO samples respectively within the experimental uncertainties (±1 emu g^{-1}, coming mainly from the uncertainty in measuring the sample mass).The M_S for undoped Fe_3O_4 nanoparticles (FO) is approximately 69.5±1 emu/g. The saturation magnetization has decreased almost linearly with the respective increase in gadolinium atomic fraction and thus can be used as a controlling parameter, wherever required. This substantial reduction in M_S with Gd doping is in agreement with the previous studies[13]. The M_S decreases roughly by 35% for the 5GdFO as compared to the FO nanoparticles. This reduction in M_S at room temperature is attributed to the substitution of sufficiently larger non-magnetic Gd^{3+} ions ($T_c \approx 292$ K) [20] at the octahedral Fe^{3+} ion sites in the inverse spinel Fe_3O_4 [12], leading to weaker superexchange interactions in GdFO samples.

The magnetic dynamics of these nanoparticles have been investigated using frequency dependent susceptibility measurements. The imaginary (out-of-phase) component of the *ac* susceptibility (χ'') *vs* temperature (T) is plotted in Figure 2(b) for all the samples, conducted at 10 Oe *ac* excitation field under zero *dc* bias conditions for six different frequencies. The well-defined peaks in the χ''*vs* T plots between 150 K to 200 K represent the superparamagnetic blocking of Fe_3O_4 nanoparticles [17]. The recorded magnetic susceptibility magnitude is the lowest for the 5GdFO sample, also consistent with the magnetic saturation measurements, described earlier.

The peak-frequency shift as a function of temperature has been estimated from these frequency dependent plots (Figure 2(b)) to understand the magnetic relaxation behavior of these nanoparticles. The behavior of an ensemble of non-interacting and single domain magnetic

nanoparticles is explained by the Néel-Brown (NB) theory under canonical approximation. The mean relaxation time for the magnetic moments of such individual nanoparticles is governed by the Arrhenius relation given by $\tau = \tau_0 \exp(E_A/k_BT)$, where k_B is the Boltzmann's constant, T is the temperature and τ_0 is the attempt time characteristic of the material and is of the order of 10^{-13}–10^{-9} s[17]. The $\ln\tau$ *vs* 1/T plots are shown in Figure 2(c). The data are fitted within the NB relaxation approximations for all these samples and the values of τ_o and E_A/k_B are summarized in Table 1.

The magnitude of τ_o was enhanced while E_A/k_B roughly lowered (although the E_A/k_B values are almost the same for 1GdFO and 2.5GdFO nanoparticles) following the increase in Gd doping percentage or an enhanced crystallite size. This increase in the value of τ_o following an increase in the particle size was also reported for hematite nanoparticles[21].The NB model suggests that $\tau_o \propto (T_B/K^3V)^{1/2}$ for ferromagnetic particles [21], where T_B is the blocking temperature, K is the anisotropy constant and V is the volume of the nanoparticle.Considering the blocking temperature, T_B, to be nearly constant for all investigated nanoparticle samples, it is observed that τ_o increases few orders of magnitude with increasing particle's size, consistent with our experimental observations.The value of $\tau_o \approx 10^{-9}$s obtained for the FO sample falls well within the accepted NB range and signifies superparamagnetic blocking in these nanoparticles. The magnetic dipolar interaction energy (E_d) existing among these nanoparticles is estimated using the relation [22, 23]:

$$E_d = \frac{\mu_o \mu^2}{4\pi a^3}\left(\frac{\pi}{4}\right)^2$$

with $\mu = m_s(\pi d^3/6)$, where μ, m_s, a and d represent the average magnetic moment, volumic saturation magnetization, average inter-particle separation and diameter of these nanoparticles respectively [23]. Considering close-packing of these nanoparticles, the magnitude of this interaction is found to be the largest, close to 0.031 eV at 300 K, for the 5GdFO nanoparticle system while it is around 0.02 eV (~ 0.017 eV for 1GdFO and 2.5GdFO, ~ 0.022 eV for FO samples) for the other nanoparticle samples. This dipolar energy signifies the magnetic interaction in an ensemble of magnetic nanoparticles, suggesting that the observed interactions are comparable with the room temperature thermal energy ~ 0.026 eV. The magneto-crystalline anisotropy constant, K, calculated for FO and 5GdFO samples using the relation $E_A = KV$, V

being the volume of the nanoparticle, are 2.5×10^4 J/m^3 and 0.45×10^4 J/m^3 respectively. Thus, K_{FO} is roughly five times larger than K_{5GdFO}, a phenomenon primarily attributed to size-dependent properties of nanoparticles [21].

The temperature dependent dielectric properties of the as-synthesized nanopowders are recorded on the cold-pressed pellets using HP 4284A Precision LCR meter integrated with a PPMS.The relative dielectric constant (ε_r) and dielectric loss corresponding to FO and 5GdFO nanoparticles with respect to temperature at three different frequencies (1kHz,100kHz,1MHz) are plotted in Figure 3(a). It has been observed that for a specific frequency, Gd doping leads to an enhancement in the magnitude of ε_r. The monotonic rise in the dielectric loss, shown in Figure 3(a), at higher temperatures (i.e. T > 200 K) is attributed to the increase in the number and root mean square speed of the thermally activated Fermi electrons. The high temperature feature observed for FO sample coincides with the ice-water transition (~273 K) , which could originate from adsorbed water molecules on the pellet's surface [24]. A low temperature (~100K) variation of the peak frequency in the dielectric loss as a function of temperature has been observed and is more prominent for GdFO as compared to the FO nanoparticles. This variation is the characteristic signature of a relaxor ferroelectric, confirming the ferroelectric nature of the undoped and GdFO samples. The temperature range for such relaxor behavior is quite high ~80 K – 130 K, suggesting the onset of ferroelectric ordering in these nano-geometrical samples may be relatively high as compared to the previously observed relaxor ferroelectric behavior in Fe_3O_4 thin film [25].

In addition, the dielectric loss peak's amplitude is frequency independent, suggesting the Debye relaxation mechanism for such ferroelectric dipoles. The local charge dipoles may arise due to the iron (or gadolinium) and oxygen ions charge distribution in these samples. These local dipolar rearrangements are driven by the thermal agitations, and their activation energy (U) can be estimated with the help of Arrhenius equation [26]:

$$f_P = f_0 e^{-U/kT},$$

where f_p is the loss peak frequency, f_0 is a constant, k is Boltzmann's constant and T is the temperature. The semi-log peak frequency data versus temperature inverse, extracted from temperature variation of the dielectric loss, is summarized in Figure 3(b), where the Arrhenius dependence had been fitted to the measured data. The estimated activation energy increased from 0.1 eV for undoped to ~0.12 eV for the 5GdFO sample. This increase is ascribed to heavier Gd^{3+}

ions substitution at relatively lighter Fe^{3+} ion sites, where heavier atom will require more energy for activating the relaxation of respective electric dipoles.

The ferroelectric polarization moments plotted in Figure 4 are obtained by integrating the measured pyrocurrent signals (shown in the insets of Figure 4) of FO and 5GdFO pellets. The measured saturation polarization values are ~ 0.04 and 0.085 μC/cm^2 for FOand 5GdFOsamples respectively. The onset of ferroelectric polarization is at ~100 K and ~130 K for FO and 5GdFO samples respectively. The observed broad ferroelectric transition (Figure 4) substantiates the relaxor characteristics for both FO and 5GdFO samples, in contrast to sharp transitions, observed in normal ferroelectrics. This is in agreement with the observed dielectric loss peaks near these temperatures for our nanoparticle samples shown in Figure 3(a) (bottom panel). The observed ferroelectric polarization for undoped nanoparticles is two orders of magnitude smaller than previously reported values [27-29]. This drastic reduction is possible in nanoparticle powder samples, where the measured ferroelectric polarization is primarily an average of the polarization vectors in all possible directions, unlike the case for better crystalline thin films [27, 29] and single crystals[28]. Moreover, the ferroelectric polarization approximately doubles its magnitude for 5GdFO sample, in contrast to the saturation magnetization, which decreased substantially. This can be understood in terms of lattice distortion created by heavier Gd^{3+} ions by substituting Fe^{3+} at octahedral sites, causing enhanced ferroelectric polarization in 5GdFO nanoparticles. Thus, in conjunction with magnetic properties, ferroelectric properties can also be tuned by substituting heavier rare earth Gd^{3+} ions at Fe^{3+}octahedral sites.

The simultaneous presence of magnetic and ferroelectric functional properties in a single phase system can be crucial for understanding spin-charge coupling. Considering the free energy (F) expansion in terms of ferroelectric polarization (P) and magnetization (M) order parameters[30],

$$F = \gamma P^2 M^2 + (\text{other higher order terms}),$$

the 'other higher order terms' are generally forbidden due to symmetry considerations (odd powered in P or M) or much weaker in magnitude (even powered in P or M) , hence are difficult to be measured[30, 31]. The scalar P^2M^2 term has been used to explain magneto-electric behavior in a number of systems [32]. Here, the effect of magnetic field on the dielectric properties of undoped and GdFO nanoparticle samples was measured at temperatures,T = 10 K, 50 K and 300 K,using a 100 kHz frequency signal. The obtained relative change in dielectric constant and loss are

plotted in Figure 5for FO and 5GdFO samples as a function of the magnetic field at different isotherms. The reference values ε_0 and D_0 are chosen as the dielectric constant and loss respectively at H=0 Oe. The observed skewness in some of the plots is attributed to the residual time drift effects in these samples. This time drift is attributed to the leakage in these samples, which led to undesired spurious magneto-capacitive signals integrated with the real signal[30], making it difficult to comment on the significance of the measured numerical values. However, the observed asymmetry in these coupling curves is the characteristic property and could be either a consequence of magnetostriction or magnetic hysteresis or both. The pure magnetodielectric system should exhibit parabolic behavior ($\Delta C/C \alpha H^2$; where C is capacitance and H is applied field)[33]. The observed non-parabolic magnetocapacitance measurements suggest the possibility of superimposed magnetostriction effect. The reported Fe_3O_4 magnetostriction value is in the order of 10^{-4}%[34], which is three orders of magnitude smaller than the observed change in the present case. However, Balaji *et al* have recently reported giant magnetostriction in the order of 10^{-1}% for magnetite nanoparticles[35]. Such large magnetostriction may affect drastically the measured magnetocapacitance and the combined magnetodielectric and magnetostriction changes in capacitance may result upon the application of the external field. The large magnetostriction may also affect the nature of measured magnetocapacitance, and thus, substantiate the observed large relative change in dielectric constant and asymmetric nature for these measurements as shown in Figure 5.The large magnetostriction in these samples may be responsible for the large change in grain size, which can be accommodated in the large pellets, used for these measurements. However, the separation of individual contributions of magnetostriction and magnetocapacitance is not possible from these experiments. The magnetocapacitance measurements also suggest a relatively weaker response for Gd doped iron oxide sample. This is attributed primarily to the reduced magnetic dipole moment of GdFO sample as compared to the undoped one, as explained earlier in the section of magnetic studies. These studies suggest strong correlation among spin, charge and lattice degrees of freedom even at room temperatures in these systems.

IV. CONCLUSIONS

In conclusion, the phase-pure undoped and different *at.%* Gd doped Fe_3O_4 multifunctional nanoparticles have been successfully synthesized using the chemical co-

precipitation route. The *dc* magnetic studies performed on these nanoparticle systems demonstrate their superparamagnetic behavior at room temperature, with saturation magnetization decreasing monotonically following an increment in Gd doping percentage. The Néel-Brown fits obtained from the temperature dependent *ac* magnetization measurements reveal that magneto-crystalline anisotropy decreases following an increase in Gd doping concentration, however, the attempt characteristic time,τ_0, has increased by two orders of magnitude in 5GdFO nanoparticles as compared to the undoped. Additionally, as observed from temperature dependent dielectric studies, these nanoparticle systems exhibit relaxor ferroelectric behavior at ~100K, where ferroelectric polarization moment has increased nearly by a factor of two for 5GdFO sample as compared to Fe_3O_4, in contrast to the observed decrease in saturation magnetization. The significant change in magnetocapacitance substantiates the strong charge-spin-lattice coupling in these samples, suggesting that these nanoparticles could possibly be used as a multifunctional multiferroic system, where external stimuli may be integrated to control the different degrees of freedom. The substitution of larger Gd^{3+} ions into the smaller Fe^{3+} sites can further be utilized as a design parameter to tailor the magnetic, ferroelectric and magnetodielectric properties in Fe_3O_4 nanoparticle systems. Also, the detailed magnetostriction measurements would be of great importance in understanding the individuals' (magnetocapacitance and magnetostriction) contribution in these systems.

ACKNOWLEDGEMENTS

This work is supported by the National Science Foundation DMR-1306449. We acknowledge useful discussions with Prof. Ratna Naik (Wayne state University) and Prof. Vaman Naik (University of Michigan). This work is dedicated to the memory of Prof. Gavin J. Lawes (Wayne State University).

References:

1. Q. A. Pankhurst, J. Connolly, S. Jones and J. Dobson,"Applications of magnetic nanoparticles in biomedicine," Journal of physics D: Applied physics, [36] R167 (2003)

2. D. L. Leslie-Pelecky and R. D. Rieke,"Magnetic properties of nanostructured materials," Chemistry of materials, [8] 1770-1783 (1996)

3. J. Liu, Y. Bin and M. Matsuo,"Magnetic Behavior of Zn-Doped Fe3O4 Nanoparticles Estimated in Terms of Crystal Domain Size," The Journal of Physical Chemistry C, [116] 134-143 (2012)

4. J. Bao, W. Chen, T. Liu, Y. Zhu, P. Jin, L. Wang, J. Liu, Y. Wei and Y. Li,"Bifunctional Au-Fe3O4 Nanoparticles for Protein Separation," ACS Nano, [1] 293-298 (2007)

5. B. Qu, X. D. Sun, J. G. Li, Z. M. Xiu, S. H. Liu and C. P. Xue,"Significant improvement of critical current density in MgB 2 doped with ferromagnetic Fe 3 O 4 nanoparticles," Superconductor Science and Technology, [22] 015027 (2009)

6. Q. Lin, J. Wang, Y. Zhong, J. Sunarso, M. O. Tadé, L. Li and Z. Shao,"High performance porous iron oxide-carbon nanotube nanocomposite as an anode material for lithium-ion batteries," Electrochimica Acta, [212] 179-186 (2016)

7. H. D. Nguyen, T. D. Nguyen, D. H. Nguyen and P. T. Nguyen,"Magnetic properties of Cr doped Fe3O4 porous nanoparticles prepared through a co-precipitation method using surfactant," Advances in Natural Sciences: Nanoscience and Nanotechnology, [5] 035017 (2014)

8. P. Drake, H.-J. Cho, P.-S. Shih, C.-H. Kao, K.-F. Lee, C.-H. Kuo, X.-Z. Lin and Y.-J. Lin,"Gd-doped iron-oxide nanoparticles for tumour therapy via magnetic field hyperthermia," Journal of Materials Chemistry, [17] 4914-4918 (2007)

9. G. H. Du, Z. L. Liu, X. Xia, Q. Chu and S. M. Zhang,"Characterization and application of Fe3O4/SiO2 nanocomposites," J Sol-Gel Sci Technol, [39] 285-291 (2006)

10. P. Hongting and J. Fengjing,"Towards high sedimentation stability: magnetorheological fluids based on CNT/Fe 3 O 4 nanocomposites," Nanotechnology, [16] 1486 (2005)

11. T.-I. Yang, R. N. C. Brown, L. C. Kempel and P. Kofinas,"Magneto-dielectric properties of polymer–nanocomposites," Journal of Magnetism and Magnetic Materials, [320] 2714-2720 (2008)

12. J. Peng, M. Hojamberdiev, Y. Xu, B. Cao, J. Wang and H. Wu,"Hydrothermal synthesis and magnetic properties of gadolinium-doped CoFe2O4 nanoparticles," Journal of Magnetism and Magnetic Materials, [323] 133-137 (2011)

13. N. Xiao, W. Gu, H. Wang, Y. Deng, X. Shi and L. Ye,"T1–T2 dual-modal MRI of brain gliomas using PEGylated Gd-doped iron oxide nanoparticles," Journal of Colloid and Interface Science, [417] 159-165 (2014)

14. R. N. Panda, J. C. Shih and T. S. Chin,"Magnetic properties of nano-crystalline Gd- or Pr-substituted CoFe2O4 synthesized by the citrate precursor technique," Journal of Magnetism and Magnetic Materials, [257] 79-86 (2003)

15. L. B. Tahar, L. S. Smiri, M. Artus, A. L. Joudrier, F. Herbst, M. J. Vaulay, S. Ammar and F. Fiévet,"Characterization and magnetic properties of Sm- and Gd-substituted CoFe2O4 nanoparticles prepared by forced hydrolysis in polyol," Materials Research Bulletin, [42] 1888-1896 (2007)

16. Y.-I. Kim, W. B. Im, M. K. Jeon, Y.-H. Lee, K.-B. Kim and K.-S. Ryu,"Preferential site of Gd in Gd-doped Fe3O4 nanopowder," Journal of nanoscience and nanotechnology, [11] 810-814 (2011)

17. S. S. Laha, R. Regmi and G. Lawes,"Structural origin for low-temperature relaxation features in magnetic nanoparticles," Journal of Physics D: Applied Physics, [46] 325004 (2013)

18. S. A. Osseni, S. Lechevallier, M. Verelst, P. Perriat, J. Dexpert-Ghys, D. Neumeyer, R. Garcia, F. Mayer, K. Djanashvili and J. A. Peters,"Gadolinium oxysulfide nanoparticles as multimodal imaging agents for T 2-weighted MR, X-ray tomography and photoluminescence," Nanoscale, [6] 555-564 (2014)

19. D. L. Thorek, A. K. Chen, J. Czupryna and A. Tsourkas,"Superparamagnetic iron oxide nanoparticle probes for molecular imaging," Annals of biomedical engineering, [34] 23-38 (2006)

20. S. M. Benford and G. V. Brown,"TS diagram for gadolinium near the Curie temperature," Journal of Applied Physics, [52] 2110-2112 (1981)

21. F. Bødker and S. Mørup,"Size dependence of the properties of hematite nanoparticles," EPL (Europhysics Letters), [52] 217 (2000)

22. C. J. Bae, S. Angappane, J. G. Park, Y. Lee, J. Lee, K. An and T. Hyeon,"Experimental studies of strong dipolar interparticle interaction in monodisperse Fe[sub 3]O[sub 4] nanoparticles," Applied Physics Letters, [91] 102502-102503 (2007)

23. S. S. Laha, R. Mukherjee and G. Lawes,"Interactions and magnetic relaxation in boron doped Mn 3 O 4 nanoparticles," Materials Research Express, [1] 025032 (2014)

24. M. Schoenherr, B. Slater, J. Hutter and J. VandeVondele,"Dielectric properties of water ice, the ice Ih/XI phase transition, and an assessment of density functional theory," The journal of physical chemistry. B, [118] 590-596 (2014)

25. M. Ziese, P. Esquinazi, D. Pantel, M. Alexe, N. Nemes and M. Garcia-Hernández,"Magnetite (Fe3O4): a new variant of relaxor multiferroic?," Journal of Physics: Condensed Matter, [24] 086007 (2012)

26. K. J. Andrew,"Dielectric relaxation in solids," Journal of Physics D: Applied Physics, [32] R57 (1999)

27. M. Alexe, M. Ziese, D. Hesse, P. Esquinazi, K. Yamauchi, T. Fukushima, S. Picozzi and U. Gösele,"Ferroelectric switching in multiferroic magnetite (Fe3O4) thin films," Advanced Materials, [21] 4452 (2009)

28. F. Schrettle, S. Krohns, P. Lunkenheimer, V. A. M. Brabers and A. Loidl,"Relaxor ferroelectricity and the freezing of short-range polar order in magnetite," Physical Review B, [83] 195109 (2011)

29. M. Ziese, P. D. Esquinazi, D. Pantel, M. Alexe, N. M. Nemes and M. Garcia-Hernández,"Magnetite (Fe 3 O 4): a new variant of relaxor multiferroic?," Journal of Physics: Condensed Matter, [24] 086007 (2012)

30. G. Lawes, T. Kimura, C. Varma, M. Subramanian, N. Rogado, R. Cava and A. Ramirez,"Magnetodielectric effects at magnetic ordering transitions," Progress in Solid State Chemistry, [37] 40-54 (2009)

31. G. Lawes and G. Srinivasan,"Introduction to magnetoelectric coupling and multiferroic films," Journal of Physics D: Applied Physics, [44] 243001 (2011)

32. T. Kimura, S. Kawamoto, I. Yamada, M. Azuma, M. Takano and Y. Tokura,"Magnetocapacitance effect in multiferroic ${\mathrm{BiMnO}}_{3}$," Physical Review B, [67] 180401 (2003)

33. A. Dixit, A. E. Smith, M. Subramanian and G. Lawes,"Suppression of multiferroic order in hexagonal ceramics," Solid State Communications, [150] 746-750 (2010)

34. C. W. Heaps,"The Magnetostriction of a Magnetite Crystal," Physical Review, [24] 60-67 (1924)

35. G. Balaji, R. A. Narayanan, A. Weber, F. Mohammad and C. S. S. R. Kumar,"Giant magnetostriction in magnetite nanoparticles," Materials Science and Engineering: B, [177] 14-18 (2012)

Table 1 τ_o and E_A/k_B values for FO, 1GdFO, 2.5GdFO and 5GdFO nanoparticle samples, estimated from the peak frequency variation as a function of temperature.

SAMPLES	τ_o (s)	E_A/k_B (K)
FO	9.6×10^{-9}	1640
1GdFO	9.4×10^{-8}	1298
2.5GdFO	1.5×10^{-7}	1305
5GdFO	8.7×10^{-7}	1002

Figure Captions:

Figure 1 (a) XRD spectra for FO, 1GdFO, 2.5GdFO and 5GdFO samples. **(b)** TEM images of FO and 5GdFO samples (color online only).

Figure 2(a) Magnetization (M) *vs* magnetic field(H) plots for FO (red), 1GdFO (green), 2.5GdFO (blue) and 5GdFO (brown) nanoparticle samples at 300 K **(b)** Out-of-phase susceptibility (χ'') *vs* Temperature (T) graph for FO, 1GdFO, 2.5GdFO and 5GdFO nanoparticle samples at six different frequencies of 500 Hz (red), 650 Hz (green), 800 Hz (blue), 950 Hz (orange), 1100 Hz (pink) and 1250 Hz (brown) under an excitation field of 10 Oe **(c)** Neel-Brown fits for FO , 1GdFO, 2.5GdFO and 5GdFO samples (color online only)

Figure 3(a). Dielectric constant (ε_r) and dielectric loss versus temperature for FO and 5GdFO samples **(b)** Semi-log straight line fits of dielectric loss peak frequencies versus temperature reciprocal for FO and 5GdFO nanoparticle samples (color online only).

Figure 4. Calculated ferroelectric polarization moment versus temperature for FO and 5GdFO samples. The measured pyrocurrent signals are included in the insets (color online only).

Figure 5. Relative change in dielectric constant and dielectric loss as a function of magnetic field for FO and 5GdFO samples (color online only).

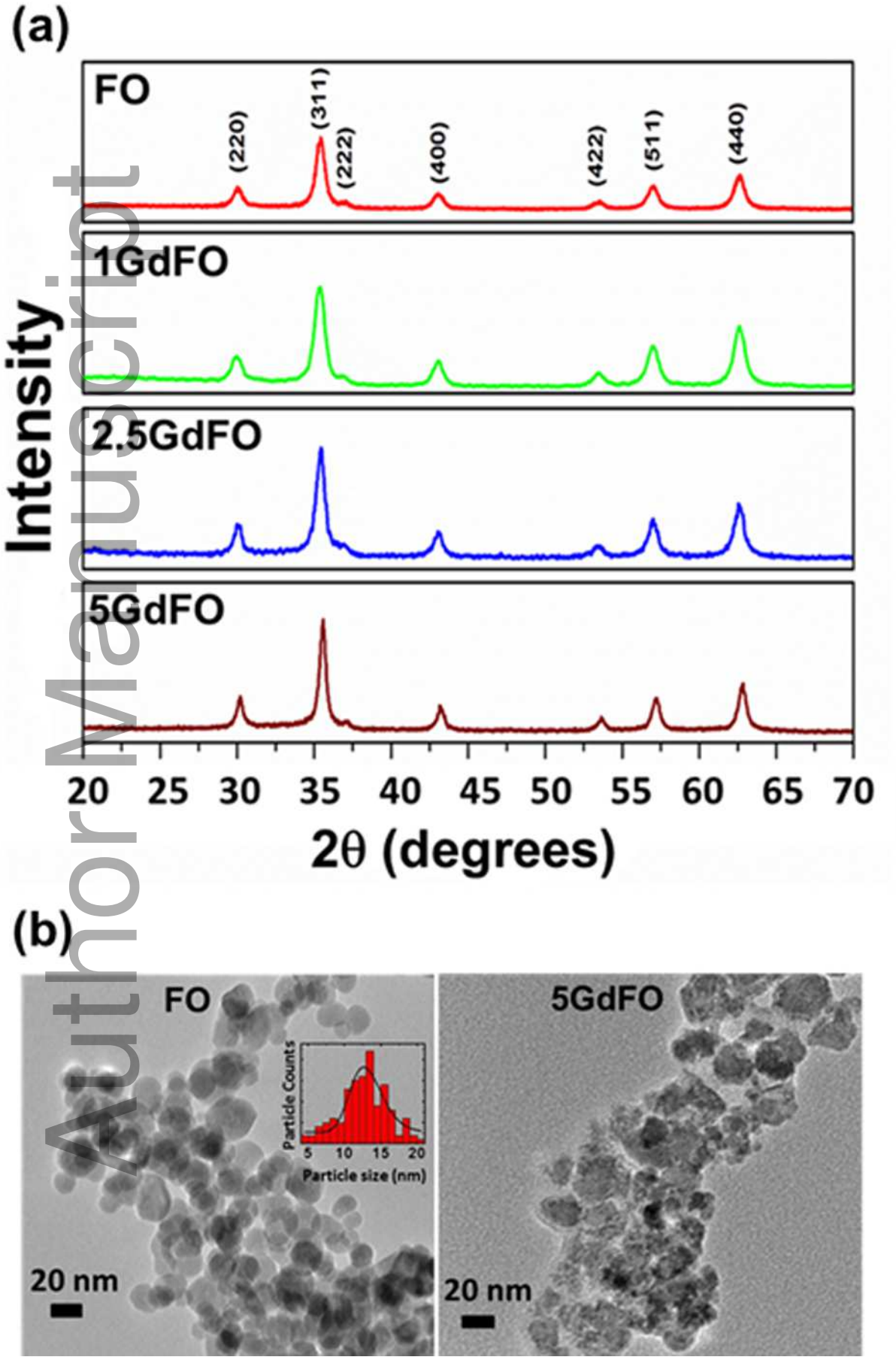

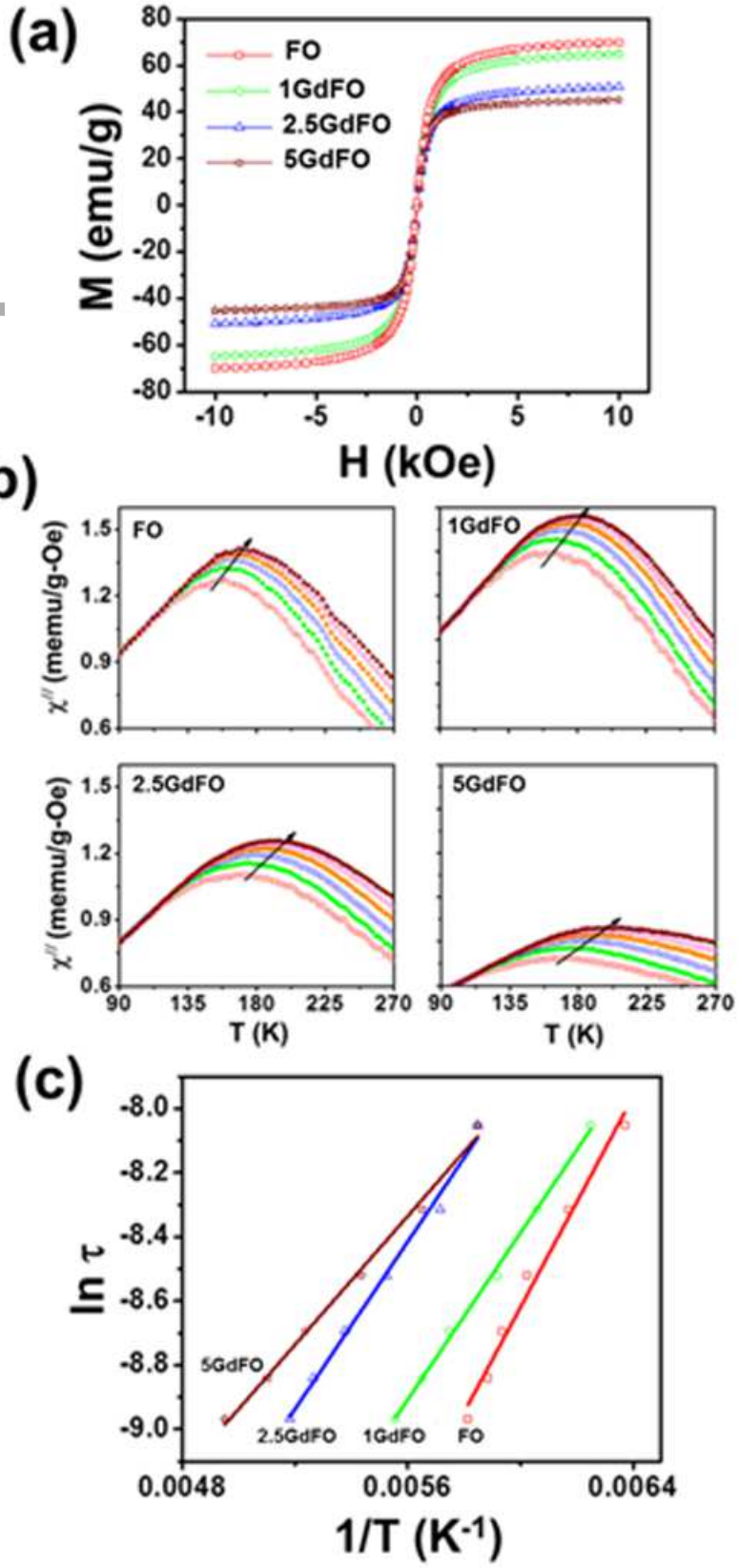

jace_14739_f2.tif

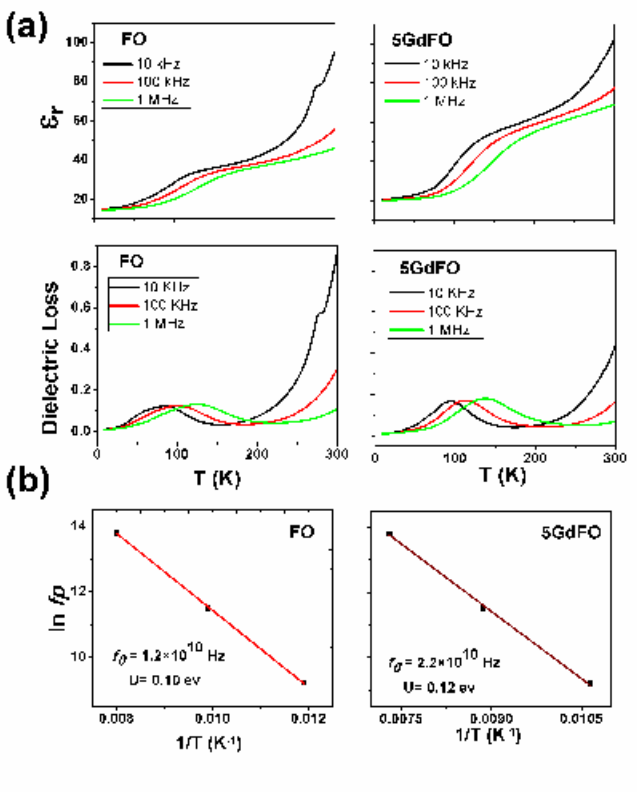

jace_14739_f3.tif

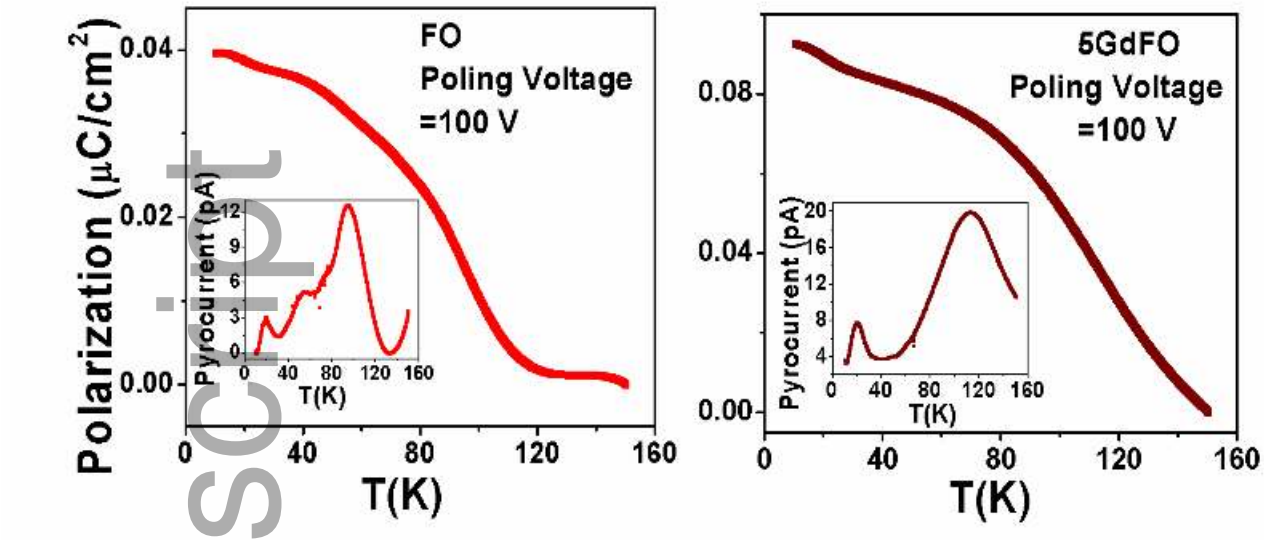

jace_14739_f4.tif

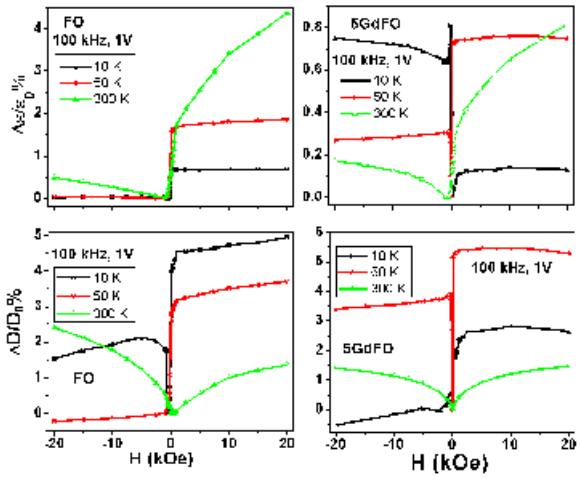

jace_14739_f5.tif